NASA TN D-30

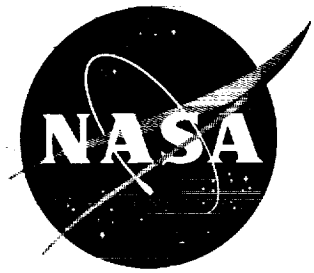

TECHNICAL NOTE
D-30

FLIGHT INVESTIGATION OF THE LIFT AND DRAG CHARACTERISTICS OF A SWEPT-WING, MULTIJET, TRANSPORT-TYPE AIRPLANE

By Ronald Tambor

Flight Research Center
Edwards, Calif.

Corrected Copy

NATIONAL AERONAUTICS AND SPACE ADMINISTRATION
WASHINGTON
September 1960

1J

NATIONAL AERONAUTICS AND SPACE ADMINISTRATION

TECHNICAL NOTE D-30

FLIGHT INVESTIGATION OF THE LIFT AND DRAG CHARACTERISTICS OF A SWEPT-WING, MULTIJET, TRANSPORT-TYPE AIRPLANE *

By Ronald Tambor

SUMMARY

The lift and drag characteristics of a Boeing KC-135 airplane were determined during maneuvering flight over the Mach number range from 0.70 to 0.85 for the airplane in the clean configuration at an altitude of 26,000 feet. Data were also obtained over the speed range of 130 knots to 160 knots at 9,000 feet for various flap deflections with gear down.

INTRODUCTION

To provide some measure of the lift and drag characteristics of an airplane having a configuration generally similar to jet transports, lift and drag data were acquired during a general flight investigation of the Boeing KC-135 airplane at the NASA Flight Research Center, Edwards, Calif. Other characteristics determined during the investigation were reported in references 1 and 2.

Data for the clean configuration were obtained in maneuvering flight within the Mach number range of 0.70 to 0.85 at an altitude of 26,000 feet. Data for the landing and take-off configurations, that is, gear down and flaps deflected, were acquired within a calibrated airspeed range of 130 knots to 160 knots at an altitude of 9,000 feet and also during take-offs and landings.

SYMBOLS

C_D drag coefficient, D/qS

C_L lift coefficient, L/qS

C_{L_α} lift-curve slope, deg^{-1} or $radians^{-1}$

*This corrected version supersedes the original version which was found to contain errors in the determination of thrust.

D	drag force along flight path, lb
F_g	gross thrust, lb
F_n	net thrust, lb
F_r	ram drag, lb
g	gravitational acceleration, ft/sec^2
L	airplane lift normal to flight path, lb
L/D	lift-drag ratio
M	Mach number
P_{T_7}	turbine-outlet total pressure, lb/sq ft
p	static pressure, lb/sq ft
q	dynamic pressure, lb/sq ft
S	wing area, 2,433 sq ft
V_c	calibrated airspeed, knots
W	airplane weight, lb
α	angle of attack, deg
δ_f	flap deflection, deg
ϵ_w	upwash due to the wings, deg
ϵ_β	upwash due to boom and fuselage, deg

Subscript:

max	maximum

EQUIPMENT

Airplane

The KC-135 airplane is a swept-wing, multijet, tanker-transport-type aircraft. For this investigation a nose boom was added and the refueling boom fins were removed. The test airplane was powered by four J57-P-43W nonafterburning turbojet engines, each with a sea-level-rated thrust of 11,200 pounds in military power. The pertinent dimensions of this airplane are listed in table I. A photograph and a two-view drawing are shown in figures 1 and 2, respectively.

Instrumentation

NASA photographic recording instruments and recording oscillographs, which were synchronized by a common timer, were used to record most of the flight data. Engine parameters were sensed by a part of the basic operational instrumentation for the J57-P-43W engines. True Mach numbers were determined from the total and static pressures measured at the end of the 13-foot nose boom. The pacer and radar phototheodolite methods were used to calibrate the airspeed system up to a Mach number of 0.90.

An angle-of-attack vane was mounted on the nose boom 10.6 feet ahead of the airplane. The indicated angle of attack was corrected for the upwash caused by the wings, fuselage, and nose boom. The correction factors shown in figure 3 were calculated by using the linearized theory presented in references 3 and 4. Because of the stiffness of the boom and the low load factors encountered during the maneuvers, corrections for boom bending were considered unnecessary. Additional angle-of-attack errors for which corrections were not made were found to be 0.5° or less by comparing the angle of attack, as corrected using the factors shown in figure 3, with the arc sin of the longitudinal accelerometer data from two runs at constant altitude and Mach number.

Other pertinent quantities were measured by standard NASA instruments.

The estimated maximum effects on drag coefficient of uncertainty in some of the measured quantities are shown in the following tabulation. These estimates are based on a dynamic pressure of 340 pounds per square foot at a pressure altitude of 26,000 feet, $C_L \approx 0.2$.

Random Errors

	ΔC_D
Normal acceleration	±0.0010
Longitudinal acceleration	±0.0010
Dynamic pressure	±0.0003

Random errors manifest themselves as scatter in the variation of drag coefficient with lift coefficient. As can be seen, the maximum actual scatter is less than estimated because the errors tend to cancel one another. Careful fairing of the data practically eliminates the effects of these errors.

Nonrandom Errors

	ΔC_D
Thrust	±0.0010
Angle of attack $\left(\text{at } C_L \approx 0.2\right)$	±0.0017

Nonrandom errors are, of course, more serious. As can be observed from the preceding tabulation, the maximum error in drag coefficient for lift coefficients near 0.2 is within ±0.0027.

PROCEDURE

Analysis

The engine net thrust was determined from the expression

$$F_n = F_g - F_r$$

The quantity F_g was based on the flight measurement of the turbine-outlet total pressure in conjunction with the ground calibration curves shown in figure 4. The quantity F_r was determined from the manufacturer's curves of compressor characteristics adjusted to flight total pressure and temperature conditions in conjunction with the flight-measured engine speed and airplane velocity.

The accelerometer method (as discussed in ref. 5) was used to compute the airplane lift and drag coefficients shown.

Tests

The high-speed data were obtained from push-down wind-up turn maneuvers during which normal acceleration varied from approximately 0.4g to 2g. The low-speed data were obtained from push-down pull-up maneuvers during which the normal acceleration varied from approximately 0.6g to 1.4g. (approaching buffet). During the maneuvers, the pilot attempted to maintain constant Mach number and engine thrust. Although both the turns and pull-ups were gradual, the amount of longitudinal control used resulted in some differences between the measured data and the data which would be obtained in a level-flight run at comparable speed and lift coefficient. For maximum lift-drag ratio, an estimate was made of this effect and is presented with the data. The test Reynolds numbers based on the mean aerodynamic chord varied from 28.2×10^6 to 56.4×10^6.

RESULTS AND DISCUSSION

High-Speed Data

The variation of drag coefficient with lift coefficient for various Mach numbers as shown in figure 5 was prepared from data obtained during push-down wind-up turns with the airplane in the clean configuration. The data presented are for the portion of the maneuver during which normal acceleration increased.

Figure 6 presents the variation of drag coefficient with Mach number for various lift coefficients. It can be observed that the drag rise $\left(dC_D/dM = 0.1\right)$ occurs at a Mach number of 0.83 for a cruise lift coefficient of 0.2. The dotted line indicates the drag coefficient at $C_L = 0$. These values were determined by extrapolation to $C_L = 0$ of curves of C_L^2 plotted against C_D.

The variations with Mach number of the maximum lift-drag ratio and the lift-drag ratios for $C_L = 0.1$, 0.2, and 0.3 are shown in figure 7. As noted previously, since the data were obtained in maneuvering flight, the longitudinal control used results in a slightly lower lift-drag ratio than would be obtained in cruising flight. By using the flight-measured control deflections, an estimate was made of this effect. The probable values of maximum lift-drag ratio for cruise are shown in the figure.

Figure 8 presents the variation of lift coefficient with angle of attack for various Mach numbers at an altitude of 26,000 feet. These

data are summarized in figure 9, which shows the effect of Mach number on the lift coefficient at zero angle of attack and also on the slope of the curve of lift coefficient plotted against angle of attack. This figure shows the usual transonic effects, as do figures 6 and 7.

Low-Speed Data

The data discussed in this section were obtained at an altitude of 9,000 feet and, therefore, do not include ground effect.

The basic low-speed lift and drag characteristics of the airplane at three flap positions with the landing gear down are presented in figure 10. Figure 10(a) shows the variation of drag coefficient with lift coefficient, and figure 10(b) shows the variation of drag coefficient with angle of attack. The increase in drag coefficient resulting from flap deflection and increasing angle of attack is apparent.

The variation of lift-drag ratio with lift coefficient for three flap deflections is shown in figure 11. The variation of maximum lift-drag ratio with flap deflection is shown in figure 12. These curves were derived from the basic data shown in figure 10.

Figure 13 shows the variation of lift coefficient with angle of attack for various flap deflections.

Figures 14(a) and 14(b) present the variation of thrust available and drag force with calibrated airspeed for various airplane weights. These curves were calculated for the airplane in trim flight at sea level using the basic data presented in figure 10. Also shown are the stall regions and the speeds at which buffeting commenced, determined from stall maneuvers shown in reference 1 and unpublished data.

Figures 15(a) and 15(b) present the variation of lift-drag ratio with calibrated airspeed for various airplane weights. These curves were also calculated for sea-level conditions from the basic data of figure 10.

Plotted in figure 16 are data from actual take-offs and landings accomplished during this investigation. The fairings represent calculated maximum lift-drag ratios based on figure 15. It can be seen that the take-offs and landings occurred at, or near, speeds corresponding to the calculated maximum lift-drag ratios.

COMPARISONS

Figure 17 shows a comparison of typical results from the present investigation with data obtained during flights reported in reference 6. At the higher Mach numbers the increased drag due to lift demonstrated by the present data results, at least in part, from the longitudinal controls used during the maneuvers, as previously discussed. There is no apparent explanation for the difference in the low-speed, 30°-flap-deflection data at the lower lift coefficients. Other differences are within the accuracy of the measurements.

H
1
1
9

High-Speed Flight Station,
National Aeronautics and Space Administration,
Edwards, Calif., April 29, 1959.

REFERENCES

1. Fischel, Jack, Butchart, Stanley P., Robinson, Glenn H., and Tremant, Robert A.: Flight Studies of Problems Pertinent to Low-Speed Operation of Jet Transports. NASA MEMO 3-1-59H, 1959.

2. Butchart, Stanley P., Fischel, Jack, Tremant, Robert A., and Robinson, Glenn H.: Flight Studies of Problems Pertinent to High-Speed Operation of Jet Transports. NASA MEMO 3-2-59H, 1959.

3. Rogallo, Vernon L.: Effects of Wing Sweep on the Upwash at the Propeller Planes of Multiengine Airplanes. NACA TN 2795, 1952.

4. Yaggy, Paul F.: A Method for Predicting the Upwash Angles Induced at the Propeller Plane of a Combination of Bodies With an Unswept Wing. NACA TN 2528, 1951.

5. Beeler, De E., Bellman, Donald R., and Saltzman, Edwin J.: Flight Techniques for Determining Airplane Drag at High Mach Numbers. NACA TN 3821, 1956.

6. Yancey, Marion H., Jr., and Martin, Reese S.: KC-135A Performance Test. AFFTC-TR-58-26, U.S. Air Force, July 1958. (Available from ASTIA as AD No. 152257.)

TABLE I.- PHYSICAL CHARACTERISTICS OF THE KC-135 AIRPLANE

General:	
Span, ft	130.83
Overall length (excluding nose boom), ft	136.25
Height, ft	38.42
Design gross weight, lb	275,000
Wing:	
Root chord, ft	28.16
Tip chord, ft	9.33
Mean aerodynamic chord, ft	20.16
Incidence, deg	2
Dihedral, deg	7
Sweep at quarter-chord line, deg	35
Aspect ratio	7.06
Stabilizer:	
Span, ft	39.67
Maximum chord, ft	17.33
Incidence (normal), deg	8
Dihedral, deg	7
Vertical fin:	
Height, ft	20.67
Base chord, ft	20.17
Angle of sweepback (leading edge), deg	36.17
Fuselage:	
Maximum width, ft	12
Maximum height, ft	17.83
Length (overall), ft	128.83
Areas:	
Wings (less ailerons), sq ft	2313.4
Wings (flaps extended), sq ft	2754.4
Ailerons (total), sq ft	119.6
Flap (total), sq ft	321.4
Stabilizers (including elevators), sq ft	500
Elevators (total including tab), sq ft	125.6
Elevator tabs (total), sq ft	11
Vertical fin (including rudder), sq ft	284
Rudder (including tabs), sq ft	87
Rudder trim tabs (total), sq ft	8.6

Figure 1.- Photograph of the Boeing KC-135 airplane. E-4123

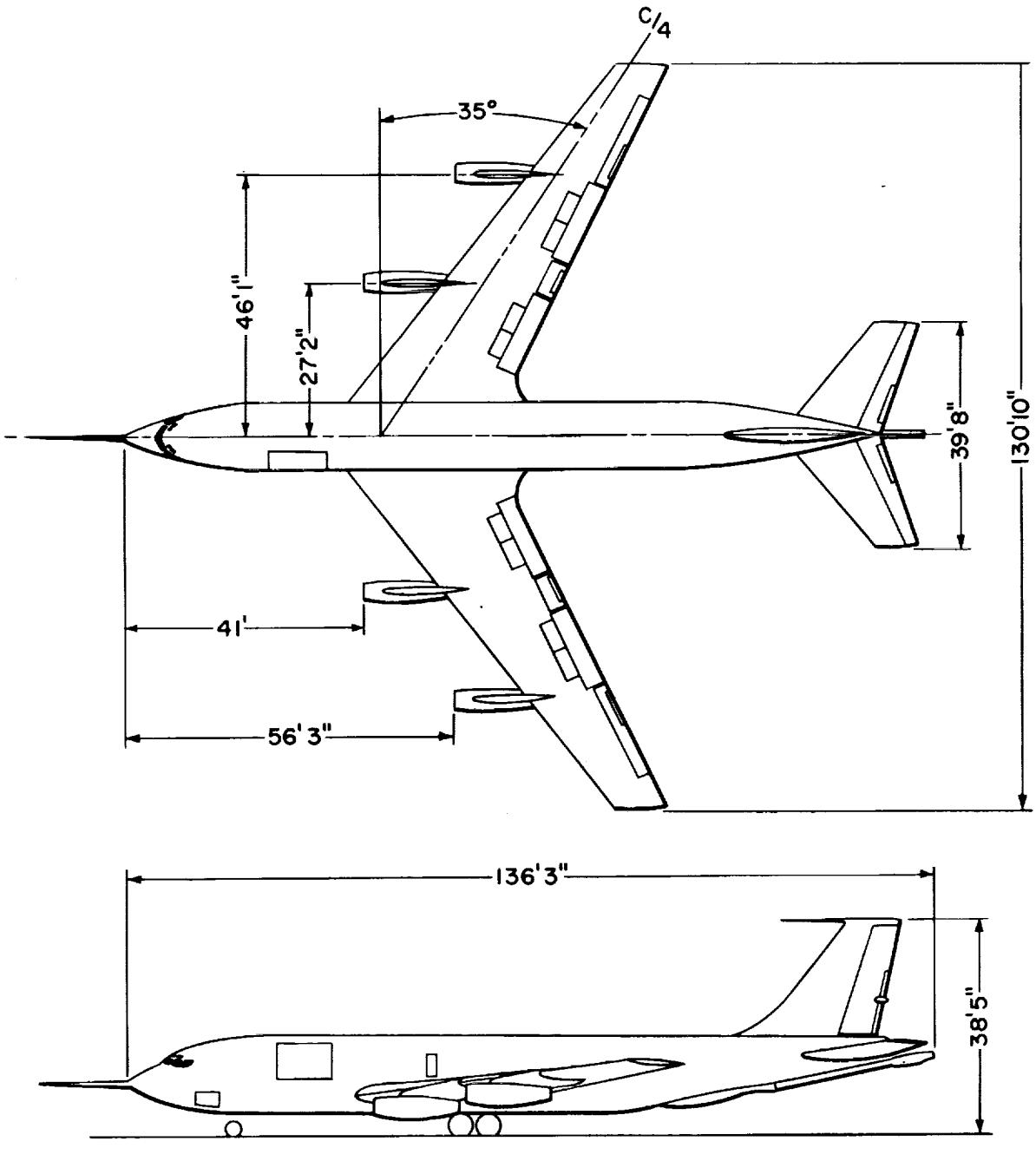

Figure 2.- Two-view drawing of the airplane.

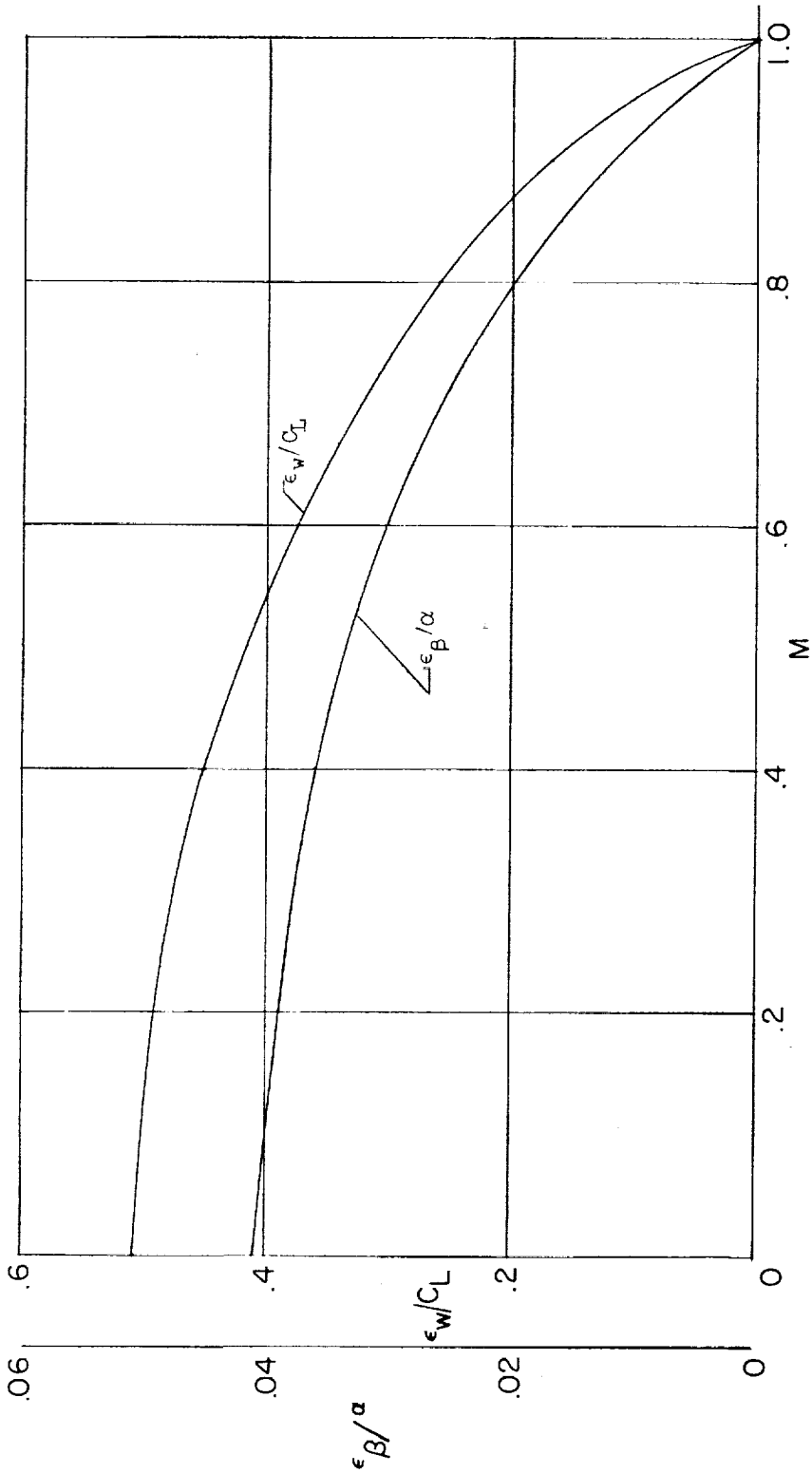

Figure 3.- Variation of upwash with Mach number at the angle-of-attack vane.

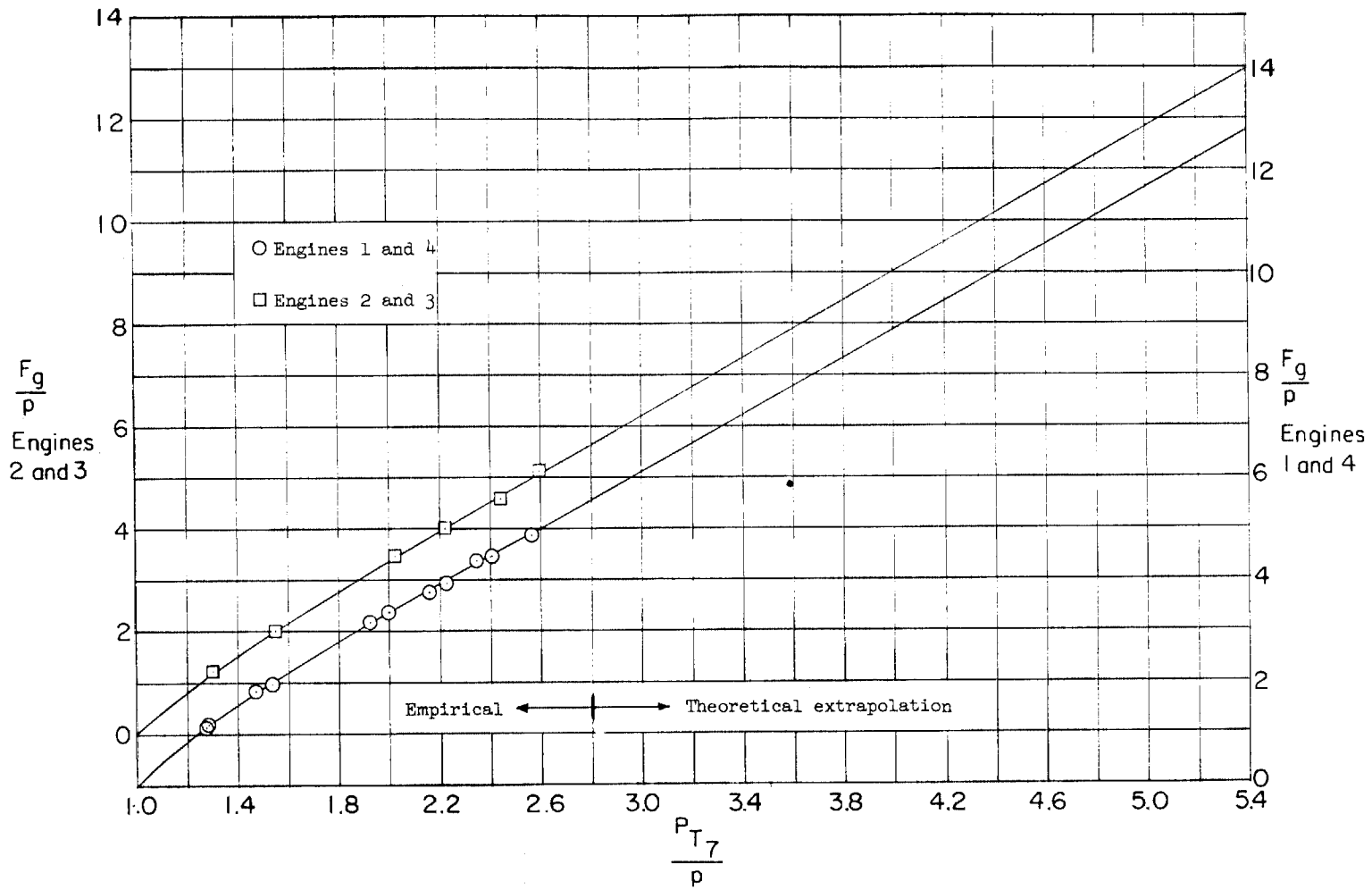

Figure 4.- Relationship of gross thrust and engine-exhaust pressure ratio obtained during a ground calibration.

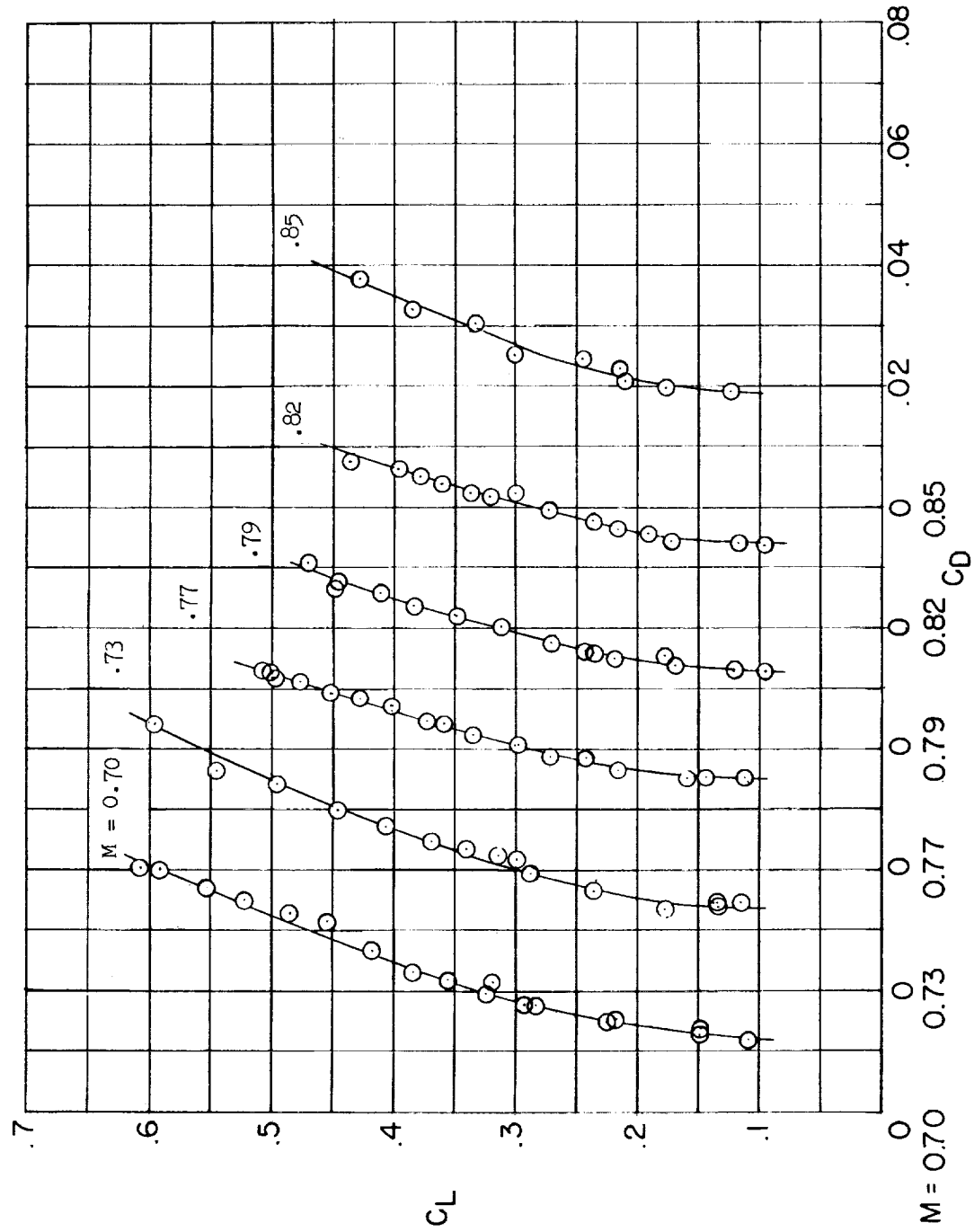

Figure 5.- Variation of drag coefficient with lift coefficient for various Mach numbers.

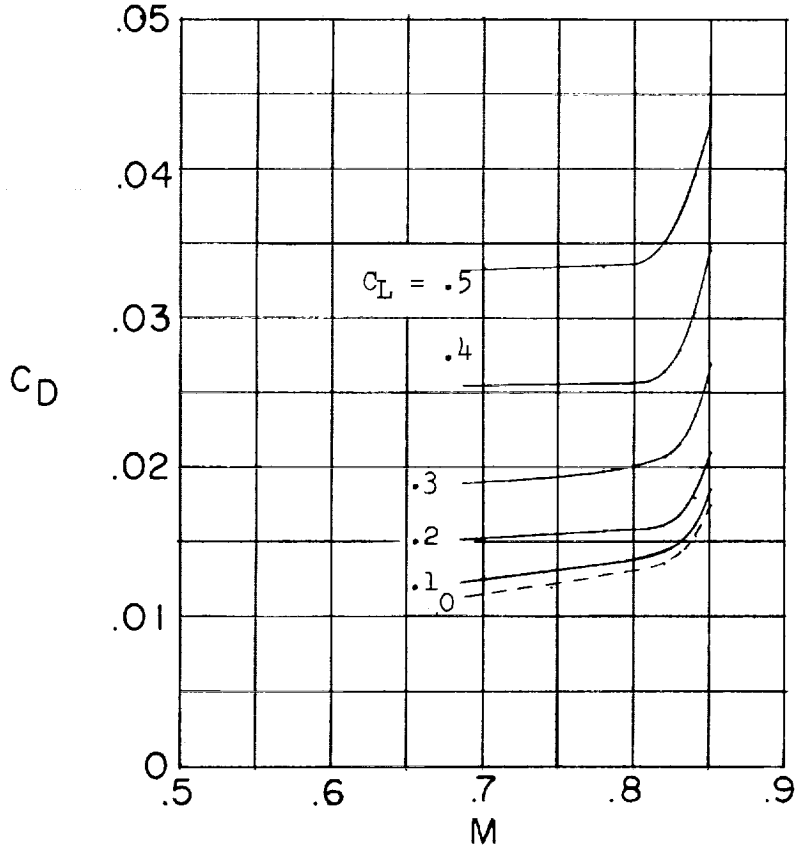

Figure 6.- Variation of drag coefficient with Mach number for various lift coefficients.

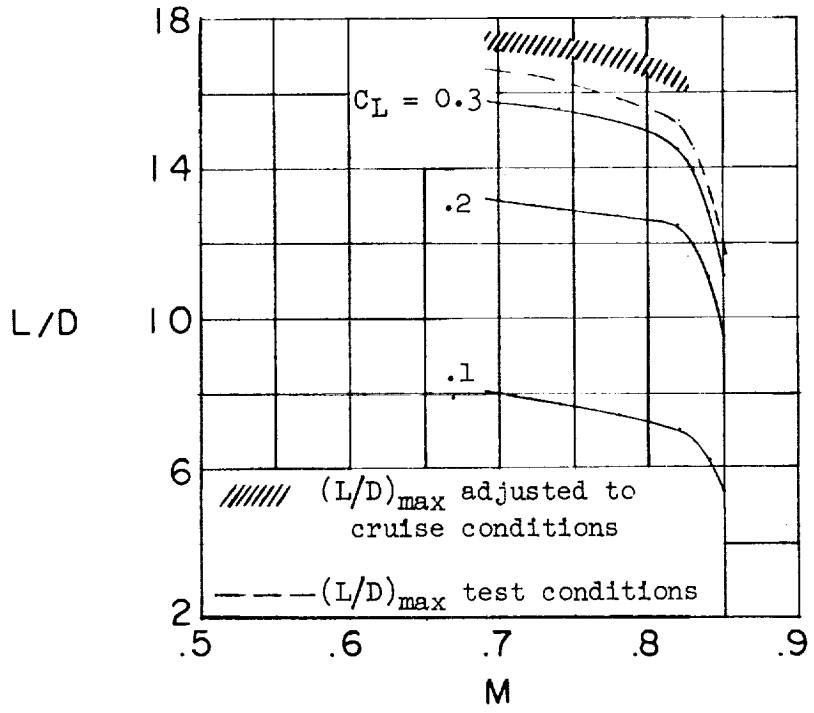

Figure 7.- Variation of lift-drag ratio with Mach number for various lift coefficients.

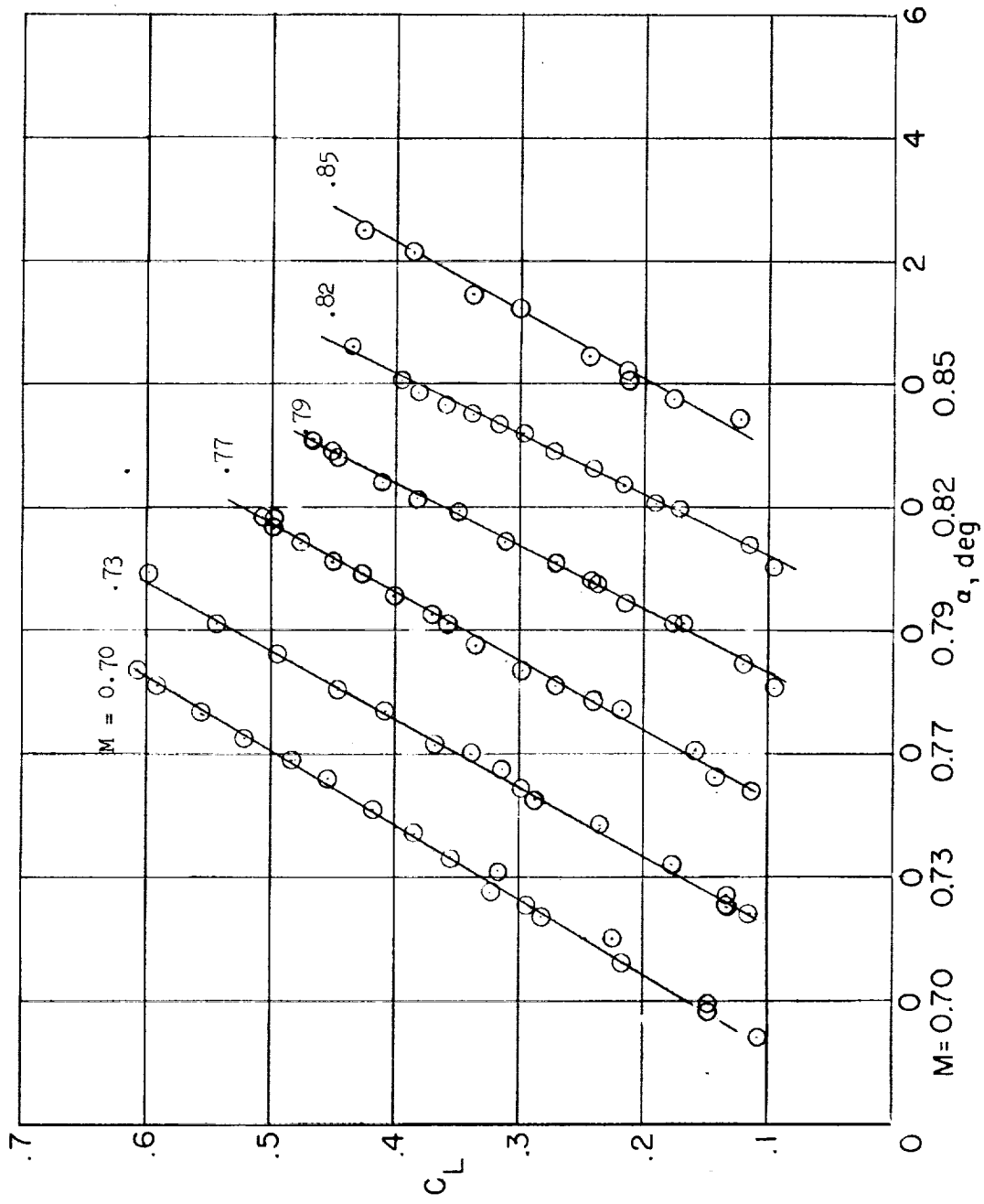

Figure 8.- Variation of lift coefficient with angle of attack for various Mach numbers.

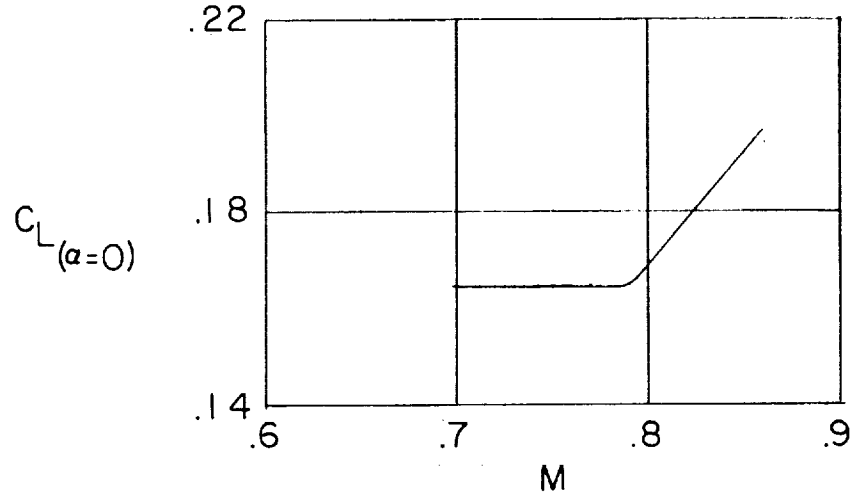

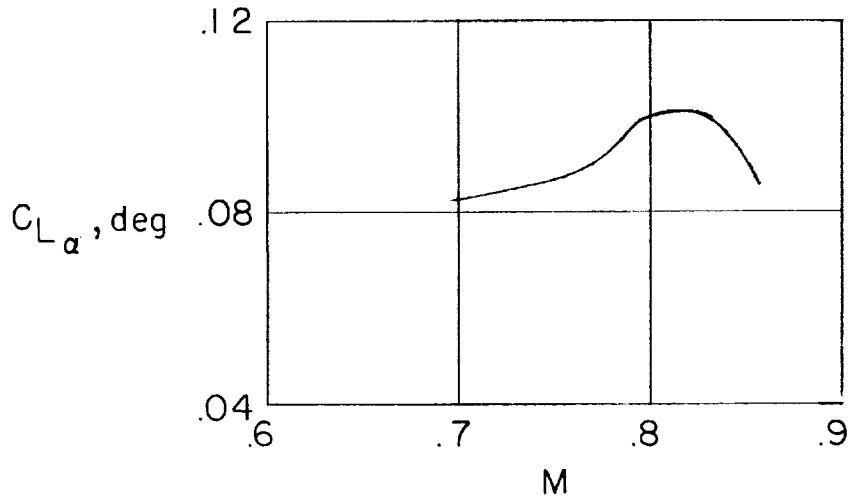

Figure 9.- Variation with Mach number of lift coefficient at zero angle of attack and of the lift-curve slope.

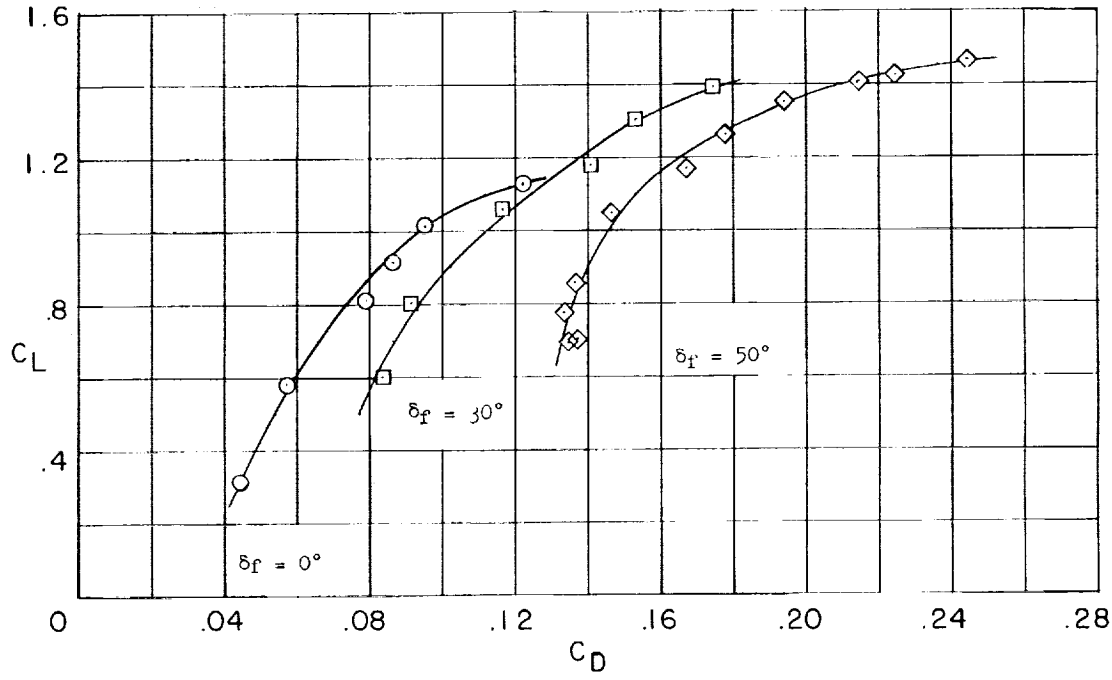

(a) Variation with lift coefficient.

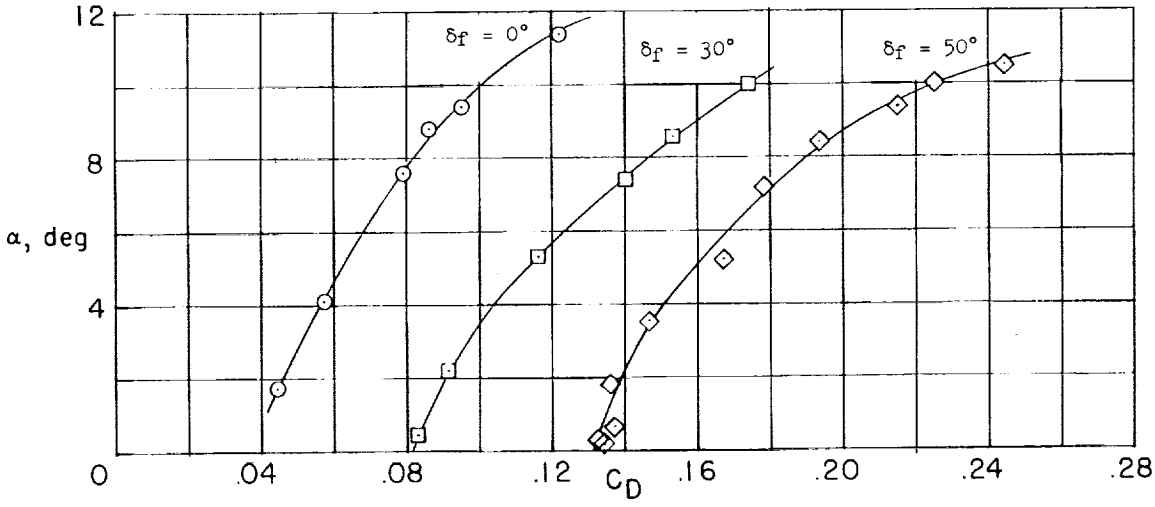

(b) Variation with angle of attack.

Figure 10.- Low-speed drag characteristics for various flap deflections with landing gear down. $M \approx 0.3$.

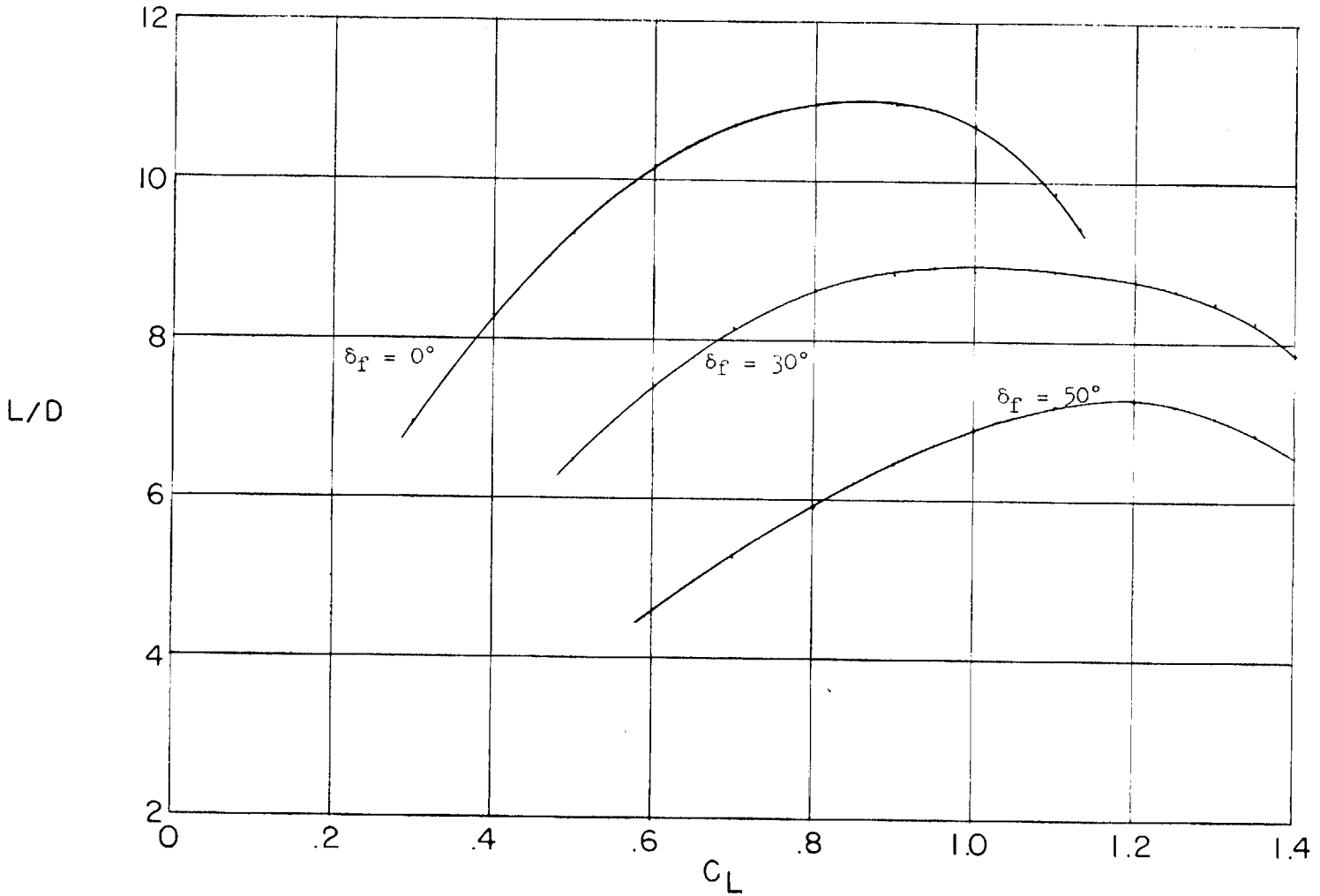

Figure 11.- Variation of lift-drag ratio with lift coefficient for various flap positions with gear down. $M \approx 0.3$.

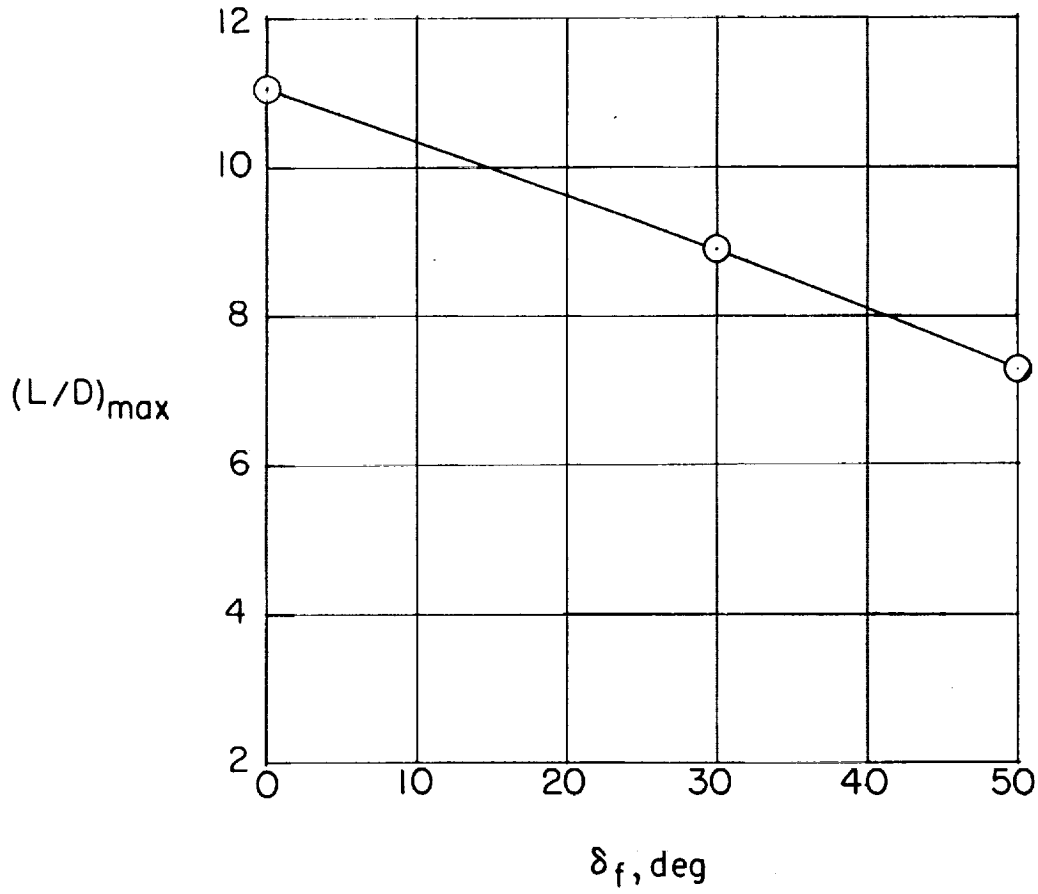

Figure 12.- Variation of maximum lift-drag ratio with flap deflection. Gear down; M ≈ 0.3.

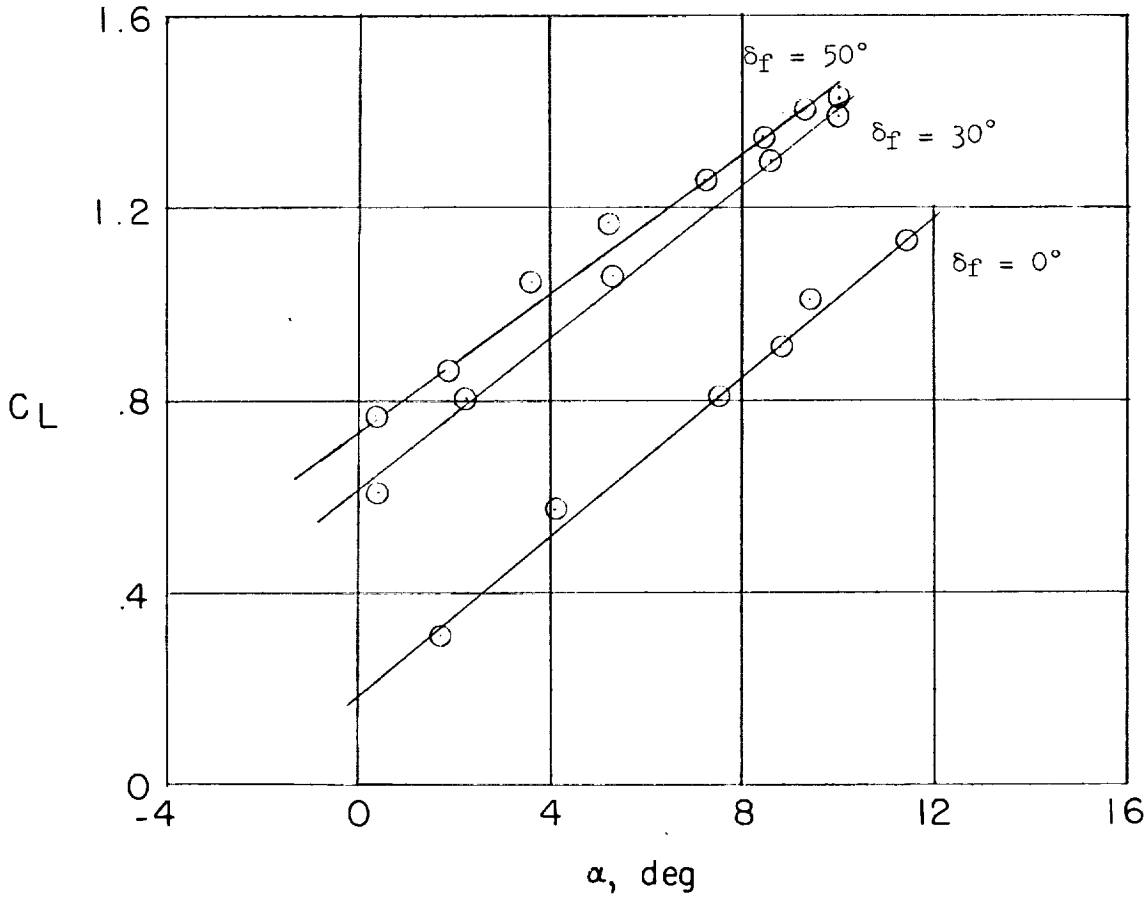

Figure 13.- Variation of lift coefficient with angle of attack for various flap deflections with gear down. M ≈ 0.3.

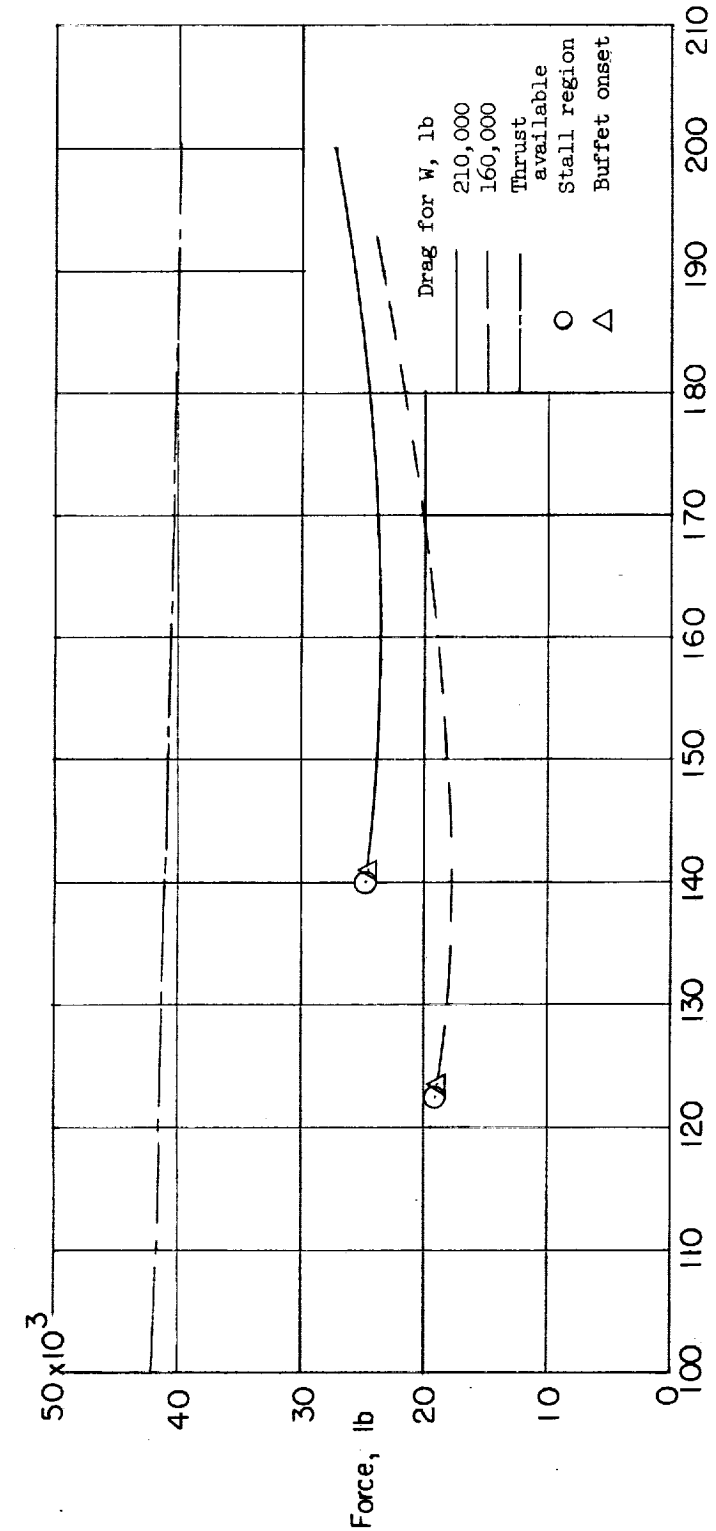

(a) 30° flap deflection, gear down.

Figure 14.- Variation of thrust available and drag with calibrated airspeed.

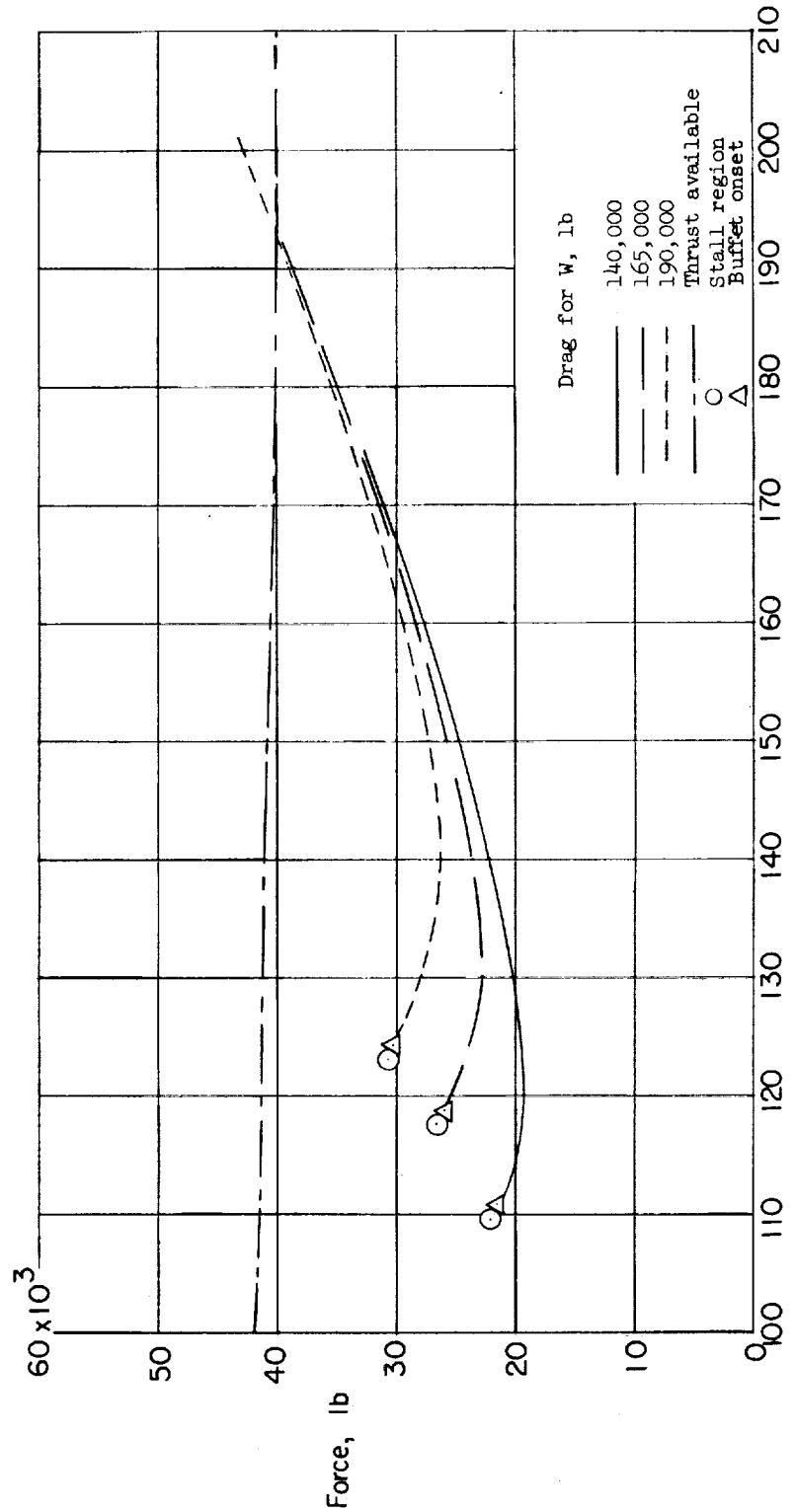

(b) 50° flap deflection, gear down.

Figure 14.- Concluded.

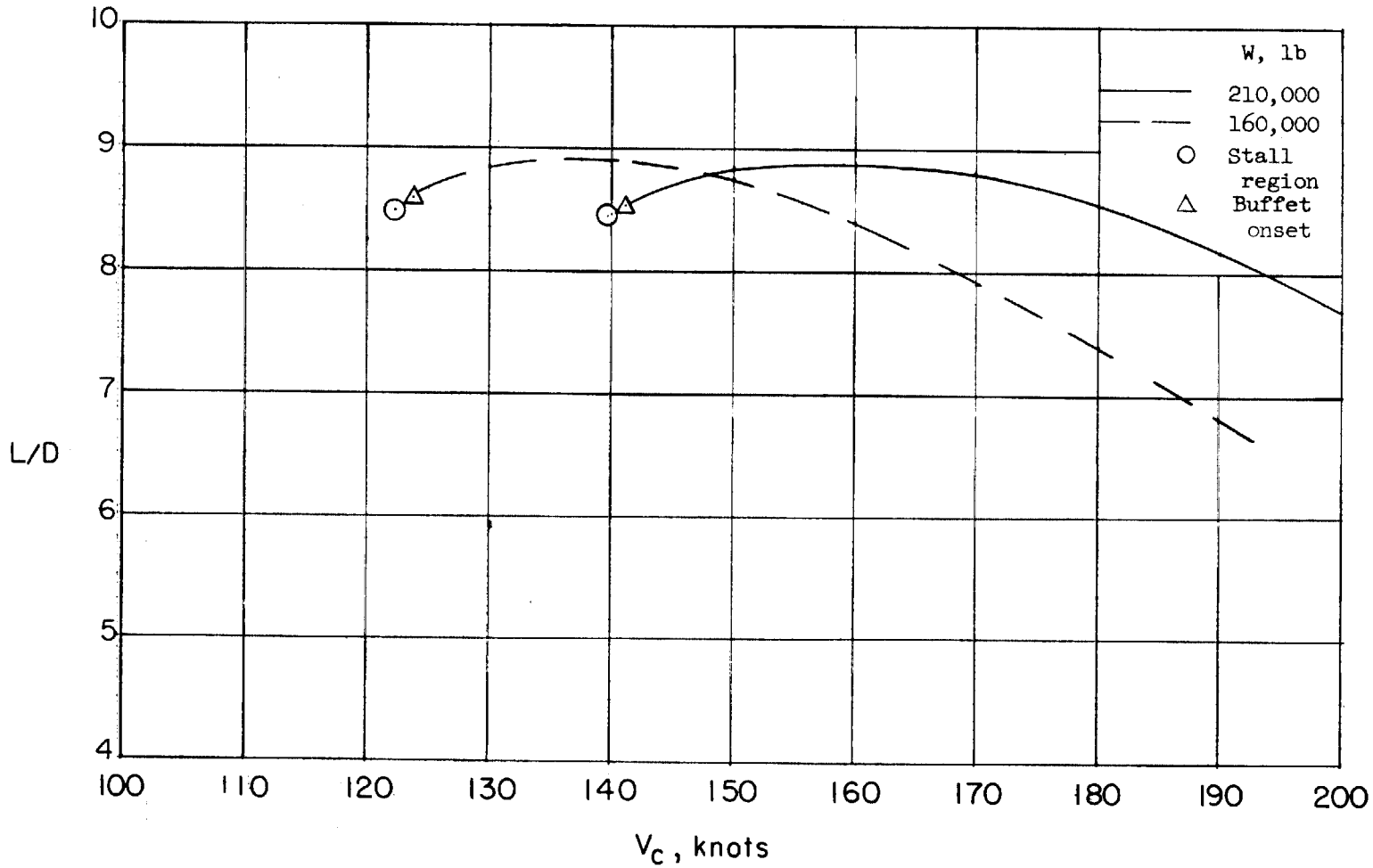

(a) 30° flap deflection, gear down.

Figure 15.- Variation of lift-drag ratio with calibrated airspeed.

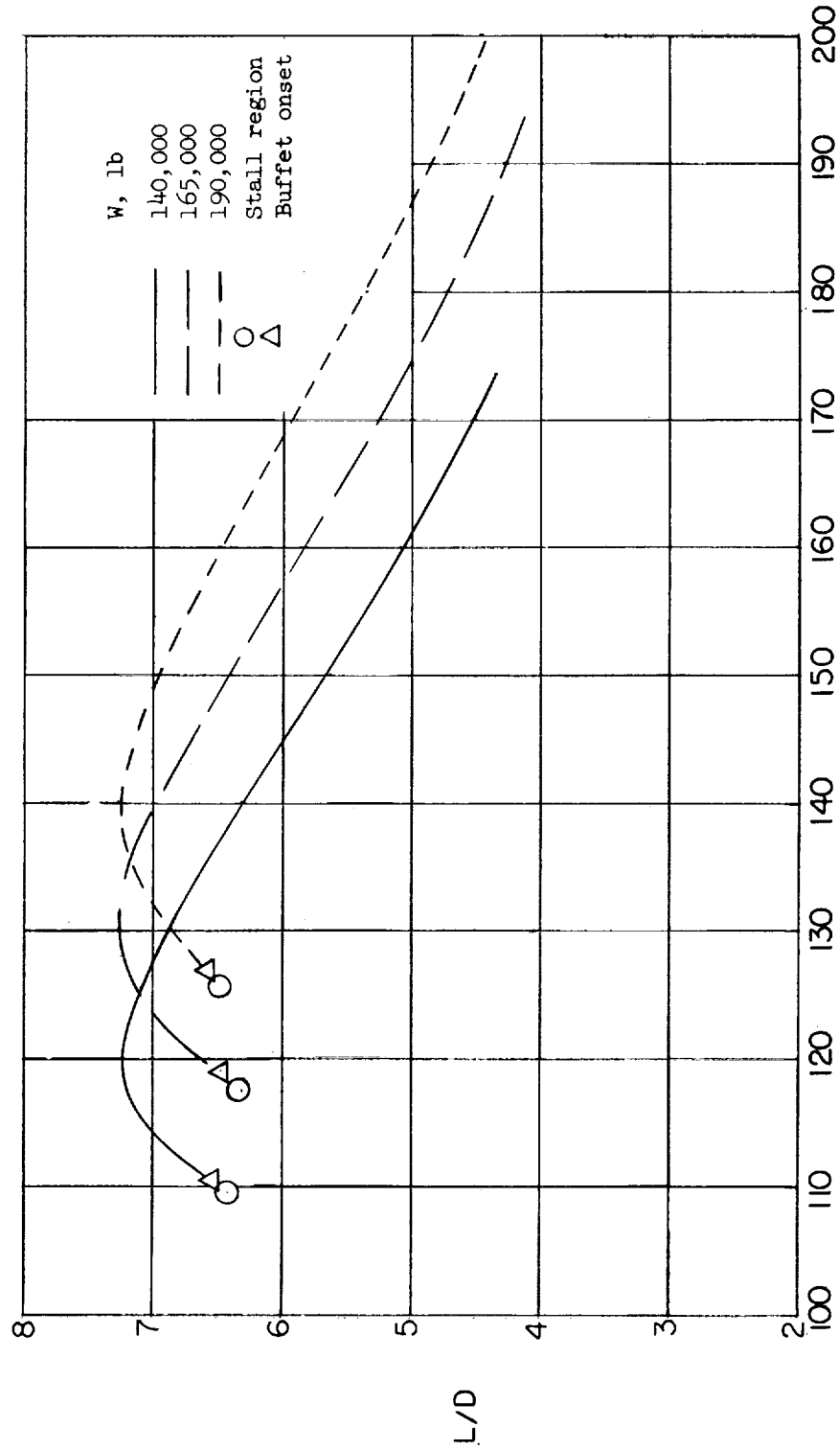

(b) 50° flap deflection, gear down.

Figure 15.- Concluded.

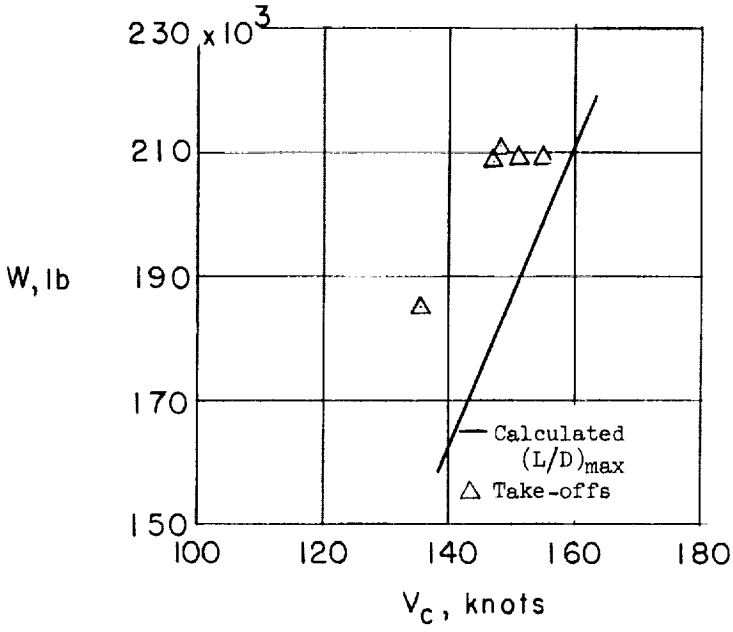

(a) 30° flap deflection.

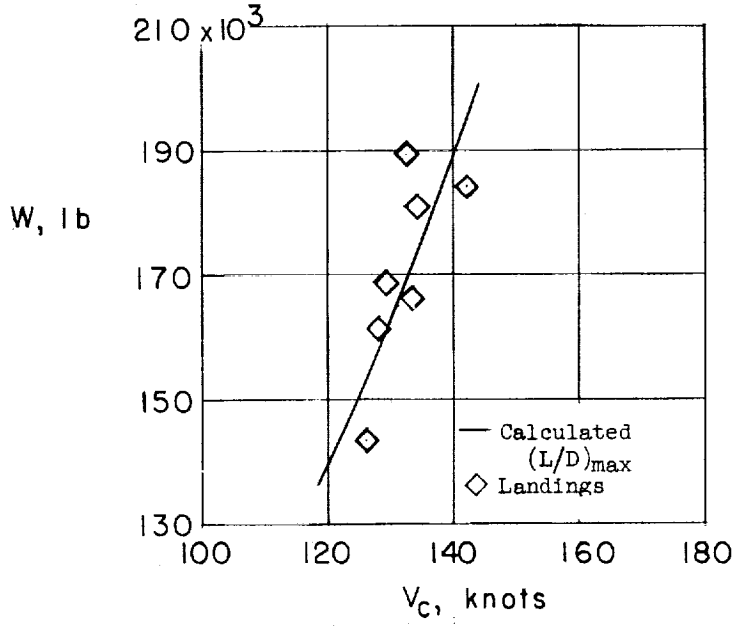

(b) 50° flap deflection.

Figure 16.- Take-offs and landing speeds for various weights.

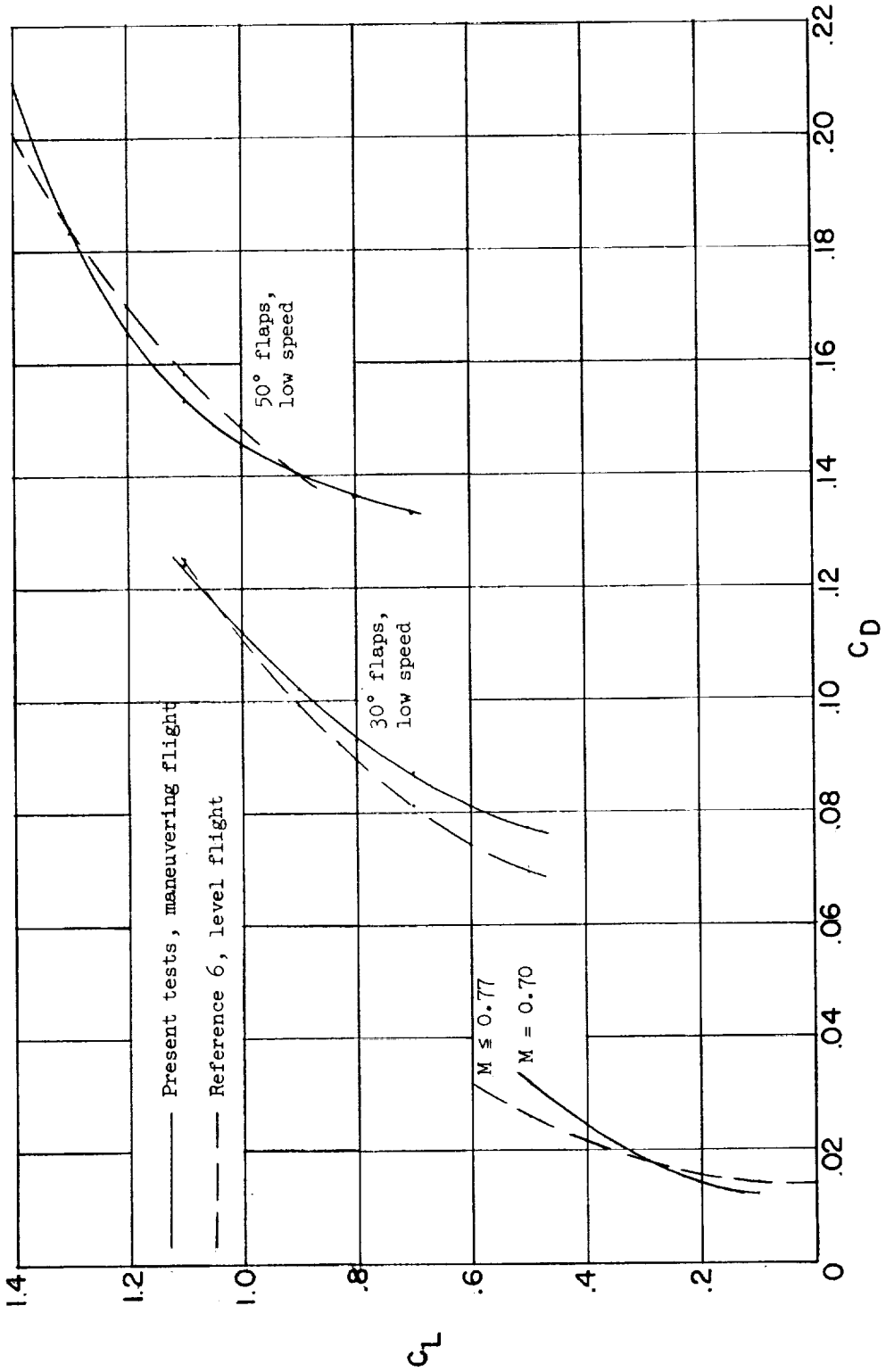

Figure 17.- Comparison of typical results from present tests and tests of reference 6.

H-119